ChemComm

COMMUNICATION

View Article Online
View Journal | View Issue

Published on 12 June 2015. Downloaded by Xiamen University on 8/17/2018 7:09:19 AM.

Cite this: *Chem. Commun.*, 2015, 51, 12016

Received 19th April 2015,
Accepted 10th June 2015

DOI: 10.1039/c5cc03241e

www.rsc.org/chemcomm

Origin of the facet dependence in the hydrogenation catalysis of olefins: experiment and theory†

Xiaojing Zhao,‡ Yun Zhao,‡ Gang Fu* and Nanfeng Zheng*

Shape-controlled Pd nanocrystals are used as model catalysts to demonstrate facet-dependent catalysis in the hydrogenation of olefins. The close packed Pd{111} shows high catalytic activity for styrene but not for *trans*-stilbene. However, the open Pd{100} facets hydrogenate both olefins. DFT calculations reveal that the hydrogenation reactivity critically depends on the stability of half-hydrogenated intermediates.

Metal nanoparticles with well-defined facets have been widely used as catalysts in a wide range of applications.[1] Fundamentally, different exposed facets have various atom arrangements, resulting in different adsorption and activation energies for various substrates.[2] For instance, the catalytic hydrogenation was readily modulated by the nanoparticles with different morphologies.[3] Experimentally, much attention has been paid to the {111} and {100} facets.[4] For instance, the turnover frequency of hydrogenation of the stilbene was revealed to be closely related to the ratio of the Pt{100} on the surface.[4a] Somorjai *et al.* showed that Pt nanocubes comprising only {100} facets can convert benzene to cyclohexane, while Pt nanocuboctahedra consisting of both the {111} and {100} facets lead to the formation of cyclohexane and cyclohexene.[4c] Li *et al.* demonstrated that by using $PtNi_2$ nanocatalysts, the reactivity of benzalacetone hydrogenation is in proportion to the percentages of exposed {111} facets, while the opposite trend was observed when starting with the nitrobenzene.[4g]

It is widely accepted that the catalytic hydrogenation follows the so-called Horiuti–Polanyi mechanism.[5] Recent theoretical studies revealed that catalytic hydrogenation might be more complex than expected.[6] Many researchers addressed that the impact of co-adsorbed hydrogen on the adsorption properties of olefins and intermediates could not be neglected.[7] For instance, Delbecq *et al.* suggested that over Pt{111}, the higher the hydrogen coverage, the lower the adsorption energy of the olefin.[8] Chizallet *et al.* proposed that under realistic conditions, both Pd{100} and Pd{111} surfaces should be saturated by hydrogen.[9] Recently, Li *et al.* showed that over a hydrogen pre-saturated Pt{111} surface, an Eley–Rideal (ER) type transition state (TS) has been identified as a more feasible pathway for the first step hydrogenation, rather than the classical Langmuir–Hinshelwood (LH) type.[10] In fact, such a mechanism is not uncommon as it has been proposed as a competitive pathway when the C=C bond is weakly adsorbed.[11]

From a traditional view, the more open facet exhibits, a higher reactivity of hydrogenation. However, if the surface were covered up by hydrogen atoms, the coordinatively unsaturated nature of different surfaces should be shadowed. In this regard, a fundamental question emerges as to which structural parameters of different exposed facets would affect the hydrogenation. Here, we explore the hydrogenation of styrene and *trans*-stilbene over Pd nanocatalysts. While Pd{111} displays good catalytic hydrogenation activity for styrene but no activity for *trans*-stilbene, Pd{100} exhibits high activity for both substrates. By means of DFT calculations, we nicely explain why open {100} facets still have higher reactivity under realistic conditions.

Hexagon-shaped Pd nanosheets with {111} as their major exposure surfaces were prepared using a CO-assisted method previously developed by our group.[12] The well-defined structure was also confirmed by transmission electron microscopy (TEM) (Fig. 1a) and high-resolution TEM (HRTEM) (inset of Fig. 1a). The presence of two basal Pd{111} planes as their major exposure surfaces makes Pd nanosheets serve as an ideal platform for investigating the reaction on the Pd{111} surface. The hydrogenation reaction of styrene was conducted at 30 °C in 1 atm hydrogen with 0.05 mg Pd nanosheets in 5 mL ethanol. The product distribution was evaluated by the gas chromatography (GC) analysis. The hydrogenation of *trans*-stilbene was carried out under the similar conditions. As shown in Fig. 1b, the conversion of styrene reached 100% within 5 min, while *trans*-stilbene almost had no conversion

State Key Laboratory for Physical Chemistry of Solid Surfaces, Collaborative Innovation Center of Chemistry for Energy Materials and Department of Chemistry, College of Chemistry and Chemical Engineering, Xiamen University, Xiamen 361005, China. E-mail: nfzheng@xmu.edu.cn, gfu@xmu.edu.cn; Web: http://chem.xmu.edu.cn/groupweb/nfzheng/index.asp

† Electronic supplementary information (ESI) available. See DOI: 10.1039/c5cc03241e

‡ X. Z. and Y. Z. contributed equally to this work.

This journal is © The Royal Society of Chemistry 2015

Published on 12 June 2015. Downloaded by Xiamen University on 8/17/2018 7:09:19 AM.

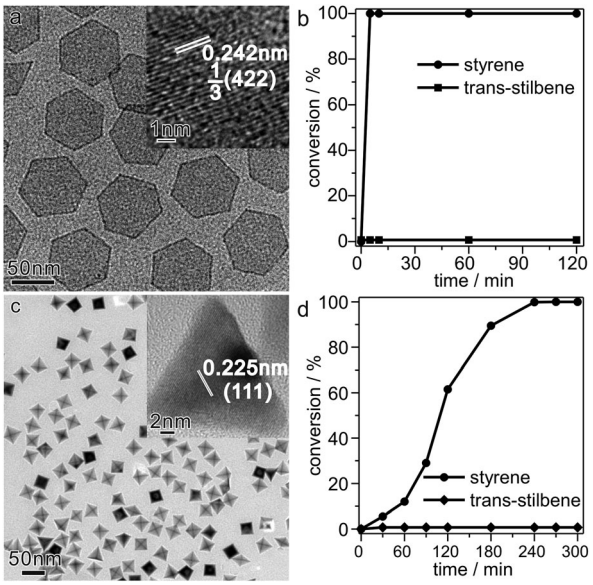

Fig. 1 TEM and HRTEM images of Pd nanosheets (a) and Pd tetrahedrons (c), respectively. Time-dependent catalytic performance of hydrogenation of *trans*-stilbene and styrene by Pd nanosheets (b) and Pd tetrahedrons (d), respectively.

even after 2 h. To further confirm such a facet-determined catalysis, Pd nanotetrahedra, also enclosed by {111} planes, were prepared and used as catalysts in the hydrogenation reactions.[3a] The obtained Pd nanotetrahedra had an average size of 37 nm (Fig. 1c). Lattice fringes with a period of 0.225 nm, consistent with the {111} lattice spacing of the fcc Pd, were clearly observed in their HRTEM image as well (inset of Fig. 1c). As shown in Fig. 1d, the Pd nanotetrahedra also exhibited a dramatic difference in the hydrogenation of styrene and *trans*-stilbene. Experimentally, the hydrogenation rate of styrene over Pd nanotetrahedra was much slower than that on Pd nanosheets, possibly due to that the surface area of the Pd tetrahedrons (33.1 $m^2\ g^{-1}$) was smaller than that of Pd nanosheets (97.2 $m^2\ g^{-1}$). Both surface areas were theoretically calculated from their geometries. Different densities of edge sites between nanosheets and tetrahedrons might also contribute to the activity difference.

Since Pd{111} is a close packed facet, one may wonder whether more open Pd{100} leads to a different catalysis behaviour. To answer this question, we also prepared Pd nanocubes with an average edge length of approximately 11 nm by using a previously reported method.[13] Our TEM studies (Fig. 2a) confirmed the successful synthesis of Pd nanocubes bound by six {100} faces. Interestingly, different from Pd nanosheets and nanotetrahedra, the prepared Pd nanocubes exhibited excellent catalytic activity in the hydrogenation of both styrene and *trans*-stilbene. As shown in Fig. 2b, the conversion of styrene reached 100% within 10 min. And *trans*-stilbene was completely converted to diphenylethane within 2 h as well. All these results clearly indicate that the hydrogenation of *trans*-stilbene on Pd is highly facet-dependent.

To deeply understand the observed facet-dependent catalysis, extensive DFT calculations were carried out. Fig. 3a shows the calculated adsorption energies for *trans*-stilbene and styrene on

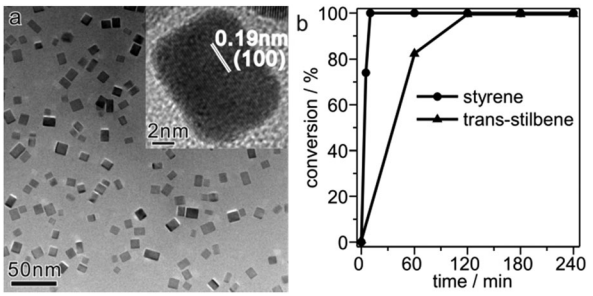

Fig. 2 (a) TEM and HRTEM images of Pd nanocubes, (b) time-dependent catalysis by Pd nanocubes.

the Pd{111} surface as a function of co-adsorbed H coverage. Both *trans*-stilbene and styrene are bound on top sites with the π bonded mode.[2,14] Our calculations revealed that with an increase in the coverage of H atoms, the adsorption energies of *trans*-stilbene increase sharply, but less so with the adsorption of styrene. However, in terms of the stability of the whole system, the energy decreased with the increase of the hydrogen coverage (Fig. 3b). When the H coverage reaches 1.0 ML, the adsorption of *trans*-stilbene becomes unstable by 0.22 eV, while the adsorption of styrene is slightly exothermic by −0.08 eV. Why the latter is still favoured? As shown in Fig. S1 (ESI†), *trans*-stilbene nearly symmetrically adsorbs on the top site with two phenyl groups away from the surface, while the styrene adsorption undergoes some tilting to minimize its steric hindrance. As reported previously,[8] the adsorption energy (ΔE_{ad}) can be decomposed into three terms, *i.e.* the surface deformation energy (ΔE_{def}(S)), the molecule deformation energy (ΔE_{def}(M)) and the interaction

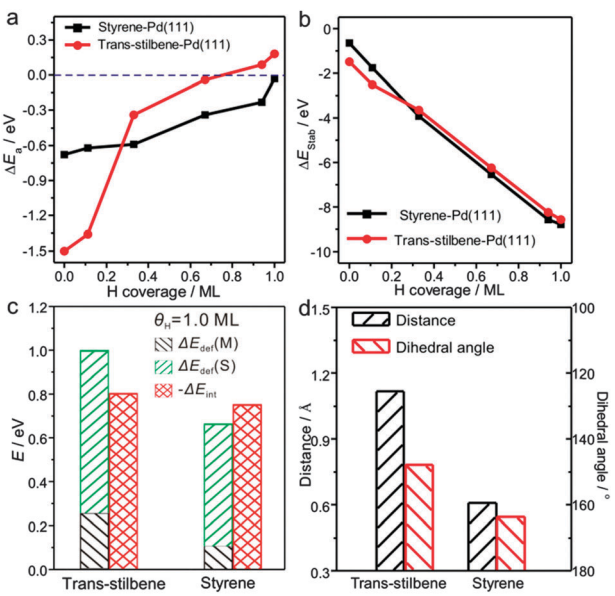

Fig. 3 (a) Adsorption energies of *trans*-stilbene and styrene interaction with Pd{111} as a function of co-adsorbed atomic hydrogen coverage (θ_H = 0, 0.11, 0.33, 0.67, 0.94, 1.00 mL), (b) the stability of the corresponding system, (c) partition of the energies of *trans*-stilbene and styrene adsorption on H-saturated Pd{111} surfaces and (d) key geometrical parameters for *trans*-stilbene and styrene bonding on hydrogen-saturated Pd{111} surfaces.

Published on 12 June 2015. Downloaded by Xiamen University on 8/17/2018 7:09:19 AM.

between the two (ΔE_{int}). Our calculations show that ΔE_{int} is approximately the same for both substrates, but there is much difference in ΔE_{def}(S) and ΔE_{def}(M). Geometrically, the *trans*-stilbene adsorption pulls the Pd atom further out of the {111} plane rather than that of styrene (1.12 Å *vs.* 0.61 Å, Fig. 3d); therefore, the former demands stronger ΔE_{def}(S) than the latter (0.76 eV *vs.* 0.57 eV). And ΔE_{def}(M) can be estimated by the dihedral angle of Ph–C=C–Ph(H), also displayed in Fig. 3d. For the adsorption of *trans*-stilbene, significant twist along the C=C bond (147.9°) consists of the relative high ΔE_{def}(M) (0.25 eV). By contrast, a smaller torsion (163.6°) of styrene adsorption leads to a small ΔE_{def}(M) of 0.11 eV.

We also investigated the adsorption behavior of the Pd{100} surface. Again, olefins are assumed to be adsorbed on the top site with the π bonded mode. On Pd{100}, the adsorption energies of *trans*-stilbene and styrene increase with the increase of the hydrogen coverage, while the opposite trends can be observed in the stability of the whole system, similar to the case of Pd{111} (*cf.* Fig. S2, ESI†). When Pd{100} is saturated by hydrogen atoms, both the *trans*-stilbene and styrene become weakly adsorbed on the surface with adsorption energies of −0.22 eV and −0.43 eV, respectively. This indicates that Pd{100} still has the ability to stabilize olefins even when the surface is completely covered by hydrogen.

According to the Horiuti–Polanyi mechanism, atomic hydrogen would be added one by one to the C=C double bond by passing through two TSs (**TS1** and **TS2**) and a semi-hydrogenated intermediate (**SHI**), as shown in Fig. 4 and Fig. S3 (ESI†). At first, we consider the hydrogenation of *trans*-stilbene on Pd{111} and Pd{100}. Fig. 4b and Table 1 summarize the optimized TS structures and the calculated energetics, respectively. For the first hydrogenation, both the LH and ER types of TSs, namely $\mathbf{TS1_{LH}}$ and $\mathbf{TS1_{ER}}$, can be located. Over Pd{111}, $\mathbf{TS1_{LH}}$ involves a barrier of 0.80 eV; while only a small barrier of 0.58 eV needs to be conquered for $\mathbf{TS1_{LH}}$ on Pd {100}. As compared with $\mathbf{TS1_{LH}}$, $\mathbf{TS1_{ER}}$ is lower in energy by 0.31 eV for Pd{111}, and 0.05 eV for Pd{100}. Interestingly, the barriers *via* $\mathbf{TS1_{ER}}$ on Pd{111} and Pd{100} are nearly the same, indicating that both facets should have a similar reactivity for the first hydrogenation.

Table 1 Calculated energies of the intermediates and the transition states along the Horiuti–Polanyi mechanism. The sum of the H saturated (θ_H = 1.0) surfaces and gas-phase olefins (styrene or *trans*-stilbene) are used as energetic reference

	Pd{111}		Pd{100}	
Pd surface	*trans*-Stilbene	Styrene	*trans*-Stilbene	Styrene
IS	0.22	−0.08	−0.22	−0.43
$\mathbf{TS1_{LH}}$	0.80	0.43	0.58	0.18
$\mathbf{TS1_{ER}}$	0.49	0.07	0.53	0.13
SHI	0.26	−0.18	−0.02	−0.41
$\mathbf{TS2_{CR}}$	0.93	0.40	1.04	0.64
$\mathbf{TS2_{CH}}$	0.92	0.43	0.47	0.14
FS	−0.36	−0.62	−0.16	−0.42

Both the LH and ER pathways were suggested to lead to the same intermediate, *i.e.* **SHI**.[10] From Table S1 (ESI†), we can see that **SHI** on the Pd{111} is less unstable than that on Pd{100} (0.26 eV *vs.* −0.02 eV). This is because the latter still has d_{z^2} type orbitals to make Pd–C bonds.[9] From the viewpoint of reverse reaction, there exists a 0.23 eV barrier from **SHI** to $\mathbf{TS1_{ER}}$ over Pd{111}, 0.33 eV less than that on Pd{100}. This indicates that over the Pd{111} surface, once **SHI** formed, it would quickly go back to *trans*-stilbene. In addition, the stability of **SHI** would influence the feasibility of the second hydrogenation. Altogether, two types of TSs for the second hydrogenation, namely $\mathbf{TS2_{CR}}$ and $\mathbf{TS2_{CH}}$, are located. The difference between them lies in their conformation. For $\mathbf{TS2_{CR}}$, the Pd–H group and the C–R group are nearly in the same plane, while in $\mathbf{TS2_{CH}}$, Pd–H···C–H is almost coplanar. Over the Pd{111} surface, the barriers of the second hydrogenation are calculated to be 0.67 eV ($\mathbf{TS2_{CR}}$) and 0.66 eV ($\mathbf{TS2_{CH}}$) with respect to **SHI**, and the overall barriers of two-step hydrogenation are as high as 0.92–0.93 eV. This can account for the fact that *trans*-stilbene has nearly no activity over Pd{111}. Over Pd{100}, the barrier from **SHI** to $\mathbf{TS2_{CH}}$ is calculated to be only 0.49 eV, indicating that the whole hydrogenation can be easily accomplished, consistent with the experiment observations.

Next, we consider the reaction mechanism of the styrene hydrogenation (Fig. S4, ESI†). As compared with *trans*-stilbene, the steric hindrance would be attenuated when styrene interacts with the surface as it has only one phenyl group. Actually, the adsorption of styrene is 0.20–0.30 eV more stable than that of *trans*-stilbene. For the first hydrogenation, calculated barriers for styrene are ~0.40 eV lower in energy than the counterparts for *trans*-stilbene, whether on Pd{111} or Pd{100}, and whether by the LH or the ER mechanism.[11] From Table 1, we can see that **SHI** and the second hydrogenation barrier for styrene are also more favourable than that for *trans*-stilbene by about 0.40 eV over either Pd{111} or Pd{100}. The overall barriers of styrene hydrogenation to phenylethane are calculated to be only 0.43 eV and 0.14 eV for Pd{111} and

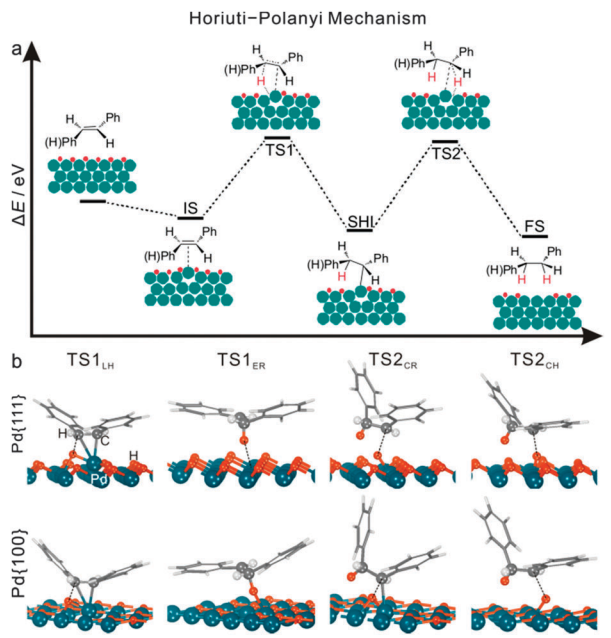

Fig. 4 (a) Schematic diagram of hydrogenation reactions by the Horiuti–Polanyi mechanism for *trans*-stilbene and styrene, (b) transition states of the hydrogenation of *trans*-stilbene adsorption on Pd{111} and Pd{100} surfaces by LH and ER types.

This journal is © The Royal Society of Chemistry 2015

Published on 12 June 2015. Downloaded by Xiamen University on 8/17/2018 7:09:19 AM.

Pd{100}, respectively, indicating that the hydrogenation of styrene on both surfaces can proceed smoothly, in accordance with experimental observations.

In conclusion, we show that the hydrogenation of C=C bonds by Pd nanocrystals is facet-dependent. Experimentally, both Pd nanosheets and Pd nanotetrahedra bound by {111} facets exhibit a high catalytic activity for styrene but no activity for *trans*-stilbene, while Pd nanocubes enclosed by {100} facets show high activity for both substrates. DFT calculations nicely explain the experimental observations and for the first time reveal that the hydrogenation reactivity critically depends on the stability of **SHI**. Even on hydrogen pre-saturated surfaces, the hydrogenation follows the Horiuti–Polanyi mechanism. For the first hydrogenation step, the **ER** type mechanism preferentially occurs such that both facets exhibit similar barriers towards a given substrate. The difference in reactivity between {111} and {100} might originate from the stability of **SHI** and its subsequent hydrogenation. A more open surface as well as the olefin with a smaller steric hindrance would help to stabilize **SHI**, thus facilitating the whole hydrogenation. On the other hand, the bulky olefin, *i.e. trans*-stilbene, forms unstable **SHI** over the compact {111} facet so that the barrier of the second hydrogenation becomes hard to be conquered. Finally, we emphasize that the interplay between theory and experiment would be necessary to realize the underlying mechanism under realistic conditions.

We are grateful for the financial support from the Ministry of Science and Technology of China (2011CB932403, 2015CB932303), the National Nature Science Foundation of China (221420102001, 21131005, 21373167, 21133004, 21333008), and the Program for Innovative Research Team in Chinese Universities (IRT_14R31).

Notes and references

1 F. Zaera, *ChemSusChem*, 2013, **6**, 1797–1820.
2 B. H. Wu and N. F. Zheng, *Nano Today*, 2013, **8**, 168–197.
3 (*a*) K. Zhou, X. Wang, X. Sun, Q. Peng and Y. Li, *J. Catal.*, 2005, **229**, 206–212; (*b*) K. Zhou and Y. Li, *Angew. Chem., Int. Ed.*, 2012, **51**, 602–613; (*c*) B. Xiao, Z. Niu, Y. G. Wang, W. Jia, J. Shang, L. Zhang, D. Wang, Y. Fu, J. Zeng, W. He, K. Wu, J. Li, J. Yang, L. Liu and Y. Li, *J. Am. Chem. Soc.*, 2015, **137**, 3791–3794.
4 (*a*) M. Cao, K. Miyabayashi, Z. R. Shen, K. Ebitani and M. Miyake, *J. Nanopart. Res.*, 2011, **13**, 5147–5156; (*b*) M. S. Jin, H. Zhang, Z. X. Xie and Y. N. Xia, *Energy Environ. Sci.*, 2012, **5**, 6352–6357; (*c*) K. M. Bratlie, H. Lee, K. Komvopoulos, P. Yang and G. A. Somorjai, *Nano Lett.*, 2007, **7**, 3097–3101; (*d*) J. Chung, C. Kim, H. Jeong, T. Yu, H. Binh do, J. Jang, J. Lee, B. M. Kim and B. Lim, *Chem. – Asian J.*, 2013, **8**, 919–925; (*e*) R. Narayanan and M. A. El-Sayed, *Nano Lett.*, 2004, **4**, 1343–1348; (*f*) E. Schmidt, A. Vargas, T. Mallat and A. Baiker, *J. Am. Chem. Soc.*, 2009, **131**, 12358–12367; (*g*) Y. Wu, S. Cai, D. Wang, W. He and Y. Li, *J. Am. Chem. Soc.*, 2012, **134**, 8975–8981; (*h*) I. Lee, R. Morales, M. A. Albiter and F. Zaera, *Proc. Natl. Acad. Sci. U. S. A.*, 2008, **105**, 15241–15246; (*i*) I. Lee, F. Delbecq, R. Morales, M. A. Albiter and F. Zaera, *Nat. Mater.*, 2009, **8**, 132–138.
5 (*a*) F. Studt, F. Abild-Pedersen, T. Bligaard, R. Z. Sorensen, C. H. Christensen and J. K. Norskov, *Science*, 2008, **320**, 1320–1322; (*b*) B. Yang, R. Burch, C. Hardacre, G. Headdock and P. Hu, *J. Catal.*, 2013, **305**, 264–276.
6 (*a*) G. Vilé, D. Baudouin, I. N. Remediakis, C. Copéret, N. López and J. Pérez-Ramírez, *ChemCatChem*, 2013, **5**, 3750–3759; (*b*) B. Yang, X. Q. Gong, H. F. Wang, X. M. Cao, J. J. Rooney and P. Hu, *J. Am. Chem. Soc.*, 2013, **135**, 15244–15250.
7 (*a*) P. Sautet and J.-F. Paul, *Catal. Lett.*, 1991, **9**, 245–260; (*b*) F. Mittendorfer, C. Thomazeau, P. Raybaud and H. Toulhoat, *J. Phys. Chem. B*, 2003, **107**, 12287–12295; (*c*) P. A. Sheth, M. Neurock and C. M. Smith, *J. Phys. Chem. B*, 2003, **107**, 2009–2017; (*d*) A. Valcárcel, A. Clotet, J. M. Ricart, F. Delbecq and P. Sautet, *Surf. Sci.*, 2004, **549**, 121–133.
8 F. Delbecq and F. Zaera, *J. Am. Chem. Soc.*, 2008, **130**, 14924–14925.
9 C. Chizallet, G. Bonnard, E. Krebs, L. Bisson, C. Thomazeau and P. Raybaud, *J. Phys. Chem. C*, 2011, **115**, 12135–12149.
10 J. Y. Li, P. Fleurat-Lessard, F. Zaera and F. Delbecq, *J. Catal.*, 2014, **311**, 190–198.
11 F. Delbecq, D. Loffreda and P. Sautet, *J. Phys. Chem. Lett.*, 2010, **1**, 323–326.
12 X. Q. Huang, S. H. Tang, X. L. Mu, Y. Dai, G. X. Chen, Z. Y. Zhou, F. X. Ruan, Z. Yang and N. F. Zheng, *Nat. Nanotechnol.*, 2011, **6**, 28–32.
13 M. Jin, H. Liu, H. Zhang, Z. Xie, J. Liu and Y. Xia, *Nano Res.*, 2010, **4**, 83–91.
14 (*a*) F. Zaera, *Phys. Chem. Chem. Phys.*, 2013, **15**, 11988–12003; (*b*) M. Neurock, V. Pallassana and R. A. van Santen, *J. Am. Chem. Soc.*, 2000, **122**, 1150–1153.